Available online at www.sciencedirect.com
ScienceDirect
Carbohydrate Polymers 71 (2008) 54–65
Carbohydrate Polymers
www.elsevier.com/locate/carbpol

Synthesis, structural characterization and properties of water-soluble *N*-(γ-propanoyl-amino acid)-chitosans

Paula Gomes [a,*], Carlos A.R. Gomes [b], Mary K.S. Batista [a,b], Luiz F. Pinto [a,b], Paulo A.P. Silva [c]

[a] *CIQUP, Departamento de Química, Faculdade de Ciências, Universidade do Porto. Rua do Campo Alegre 687, P-4169-007 Porto, Portugal*
[b] *LAQUIPAI, Departamento de Química, Faculdade de Ciências, Universidade do Porto. Rua do Campo Alegre 687, P-4169-007 Porto, Portugal*
[c] *CIEA, Instituto Superior de Engenharia do Porto. Rua Dr. António Bernardino de Almeida 431, 4200-072 Porto, Portugal*

Received 1 March 2007; received in revised form 27 April 2007; accepted 8 May 2007
Available online 17 May 2007

Abstract

Water-soluble peptide-chitosans were obtained by reaction of low-molecular-weight chitosan, having a low degree of acetylation, with peptide substituents under mild conditions. These peptide substituents were prepared by standard peptide chemistry from 3-bromopropanoic acid and *tert*-butyl esters of the α-amino acids glycine and phenylalanine. The structure of the new peptide-chitosan polymers was confirmed by proton nuclear magnetic resonance and infrared spectroscopy. The thermotropic and morphological properties of both the new peptide-chitosans and two other analogues, derived from valine and aspartic acid [synthesis reported in Batista, M. K. S., Pinto, L. F., Gomes, C. A. R., & Gomes, P. (2006). Novel highly soluble peptide-chitosan polymers: Synthesis and spectral characterization. *Carbohydrate Polymers, 64*, 299–305], were evaluated by differential scanning calorimetry and scanning electron microscopy, respectively. As compared to the parent unmodified chitosan, the four peptide-chitosans had higher thermosensitivity, porosity and water-holding capacity, and such effects increased with the hydrophilicity of the peptide ligands. The acid-base properties of the four peptide-chitosans were also evaluated by potentiometric techniques and reflected the influence of the inserted ligands on the polymers' acidity constants. It was also possible to confirm the polymers' solubility over the 2–10 pH range. Overall, these polymers present physico-chemical properties that make them promising candidates for the design of novel drug delivery systems.

Keywords: Chitosan; DSC; Drug delivery; Peptide; Potentiometry; SEM; Water soluble

1. Introduction

Biodegradable polymers derived from renewable resources have recently generated much interest for diverse pharmaceutical applications, such as drug transport and controlled release *in vivo* (Aiping, Jianhong, & Wenhui, 2006; Atyabi, Majzoob, Iman, Salehi, & Dorkoosh, 2005; Lin et al., 2005; Liu, Hsu, Su, & Lai, 2005; Ruel-Gariépy et al., 2004; Tapia et al., 2004; Thierry et al., 2005; Van der Merwe, Verhoef, Kotzé, & Junginger, 2004). Chitosan (CT), a copolymer of glucosamine and *N*-acetylglucosamine, is a non-toxic, biodegradable and biocompatible material that has been used for several biomedical purposes from gene therapy to suture and wound healing materials, vascular grafts and cartilage regeneration, among many others (Berger, Reist, Mayer, Felt, & Gurny, 2004; Berger et al., 2004; Chandy & Sharma, 1992; Danielsen, Vårum, & Stokke, 2004; Gupta & Ravikumar, 2000; Iwasaki et al., 2004; Mansouri, Lavigne, Corsi, Benderdour, & Beaumont, 2004; Mi, Sung, & Shyu, 2002; Wong et al., 2006; Zhu, Ming, & Jian, 2005). Some of the most appealing characteristics of CT are its bioadhesive properties and its ability to promote cell proliferation and, consequently, tissue regeneration (Berger et al., 2004). These properties

* Corresponding author. Tel.: +351 226082863; fax: +351 226082959.
E-mail address: pgomes@fc.up.pt (P. Gomes).

0144-8617/$ - see front matter © 2007 Elsevier Ltd. All rights reserved.
doi:10.1016/j.carbpol.2007.05.015

of CT are enhanced upon decreasing the polymer's degree of acetylation (Amaral, Lamghari, Sousa, Sampaio, & Barbosa, 2005; Amaral, Sampaio, & Barbosa, 2005; Berger et al., 2004) and are of outmost importance for biomedical engineering. Further, owing to its particular structure and self-assembly properties, CT has proved to be a useful excipient in the pharmaceutical industry (Bernkop-Schnürch, 2000; Bernkop-Schnürch & Kast, 2001; Janes, Calvo, & Alonso, 2001; Krauland, Guggi, & Bernkop-Schnürch, 2006; Takeuchi et al., 2005). Notwithstanding, the poor solubility of chitosan in both water and current organic solvents limits its effective utilization in this field. One of the reasons for the intractability of chitosan lies in its rigid crystalline structure that is related with the acetamido and primary amino groups that induce relevant conformational features through intra- and/or intermolecular hydrogen bonding (Nishimura, Kohgo, Kurita, & Kuzuhara, 1991). Replacement of one, or both, primary amino group's hydrogens by other substituents, through suitable chemical modifications, is a possible means for partial destruction of its rigid crystalline structure, increasing the polymer's solubility in aqueous or organic media (Liu, Desai, Chen, & Park, 2005). Numerous efforts have been made to prepare functional and soluble derivatives of chitosan (Delben, Gabrielli, Muzzarelli, & Stefancich, 1994; Kurita, Ikeda, Yoshida, Shimojoh, & Harata, 2002; Muzzarelli, 1988; Muzzarelli, Tanfani, & Emanuelli, 1984; Skorik, Gomes, Vasconcelos, & Yatluk, 2003). Thus, chemical modifications have been carried out on the chitin and chitosan glucopyranoside ring, conferring to the new materials surprising properties and additional possibilities of engaging in a wide range of chemical reactions (Holappa et al., 2004, 2005; Holappa, Nevalainen, Soininen, Másson, & Järvinen, 2006).

We are devoted to the development of different strategies for *in vivo* transport and controlled release of drugs that are prone to be rapidly inactivated in the first-pass metabolism (Araújo et al., 2005; Chambel et al., 2006; Gomes et al., 2004; Santos et al., 2005). The development of chitosan-based materials as potential vehicles for those drugs is one of such strategies. So, new water-soluble chitosan derivatives have been previously prepared in our group, namely, several *N*-(2-carboxyethyl)-chitosans (Skorik et al., 2003), and two peptide-chitosans (PC), *N*-(γ-propanoyl-valin)-chitosan and *N*-(γ-propanoyl-aspartic acid)-chitosan (Batista, Pinto, Gomes, & Gomes, 2006). The potential applications of these polymers as antioxidant and antimutagenic agents (Kogan et al., 2004) as well as metal chelating agents (Skorik et al., 2005) have also been studied. The present paper describes the preparation and structural characterization of two additional PC derivatives, *N*-(γ-propanoyl-glycine)-chitosan and *N*-(γ-propanoyl-phenylalanine)-chitosan, which were thoroughly characterized together with the two PC previously reported (Batista et al., 2006) to assess their physico-chemical properties and conclude about their potential interest for drug delivery *in vivo*.

2. Experimental

2.1. Materials

Low molecular weight ($M_W \sim 150$ kDa) chitosan from coarse ground crab (Ref. 44.886-9, Aldrich) was used, having a 10% degree of acetylation (DA = 10%) as determined by ^{1}H NMR and 5.4 mmol N/g as determined by elemental analysis, *i.e.*, 4.86 mmol of free $-NH_2$ groups per gram of polymer. 3-Bromopropanoic acid, *N*,*N*′-dicyclohexylcarbodiimide (DCCI), *N*,*N*′-diisopropylcarbodiimide (DIPCDI), $CDCl_3$, D_2O, DCl, anhydrous trifluoroacetic acid (TFA) and common organic solvents (*p.a.* quality) were all from Sigma–Aldrich. Glycine-, L-phenylalanine-, L-valine-*tert*-butyl ester hydrochlorides, and L-aspartic acid β-*tert*-butyl α-*tert*-butyl diester hydrochloride, were all from Bachem (Switzerland). Thin layer chromatography (TLC) plates (aluminium foil covered with 0.25 mm thick silica gel 60, F_{254}) were from Merck (Germany), and silica gel for column chromatography (Chromagel, pH 7, 35–70 μm, 550 m^2/g) was from SDS (France).

2.2. Synthesis

2.2.1. Peptide ligands

The peptide ligands were prepared as previously described (Batista et al., 2006), by condensation (Scheme 1) of 3-bromopropanoic acid with the *tert*-butyl esters of glycine or L-phenylalanine, by the carbodiimide (DCCI or DIPCDI) method (Gomes et al., 2004). Briefly, the relevant amino acid *tert*-butyl esters, purchased as hydrochloride salts, were obtained as free amines (free α-amino group) after neutralization of the hydrochloride (29.5 mmol) with aqueous Na_2CO_3 at 30% until pH 11, followed by extraction with 5 × 20-mL dichloromethane (DCM), pooling of the organic layers, drying over anhydrous $MgSO_4$ and evaporating to dryness. The L-amino acid *tert*-butyl esters were thus isolated as yellow oils with yields range between 72% and 92%. These compounds were dissolved in DCM (100 mL), then 3-bromopropanoic acid (29.5 mmol) was added and the solution was stirred in an ice-water bath for 30 min. Then, a suitable carbodiimide (DCCI or

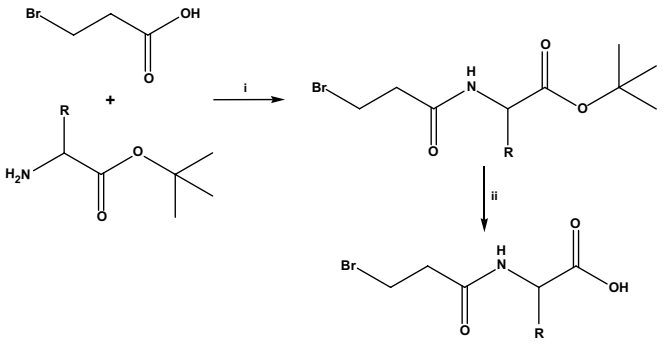

Scheme 1. Synthetic route to the peptide ligands: (i) DCCI or DIPCDI, DCM, r.t. (ii) TFA, r.t.; R = amino acid side chain.

DIPCDI, 32.5 mol) in 10% excess was slowly added to solution, which was kept at 0 °C for more 2 h. The reaction was allowed to proceed at room temperature for 48 h, with periodic monitoring by TLC. The solid phase formed was removed by suction filtration and identified as the carbodiimide-derived urea (DCU or DIU). The filtrate was evaporated to dryness and the oily residue dissolved in the minimum amount of warm acetone; the resulting solution was stored overnight at 4 °C and the additional urea precipitate was again removed by suction filtration. The filtrate was evaporated to dryness and the residue submitted to column chromatography on silica-gel, using 20:1 (v/v) DCM/acetone as eluant. The N^{α}-(3-bromopropanoyl)amino acid *tert*-butyl esters were isolated as yellow oils in 50–78% yields and their structure confirmed by ^{1}H and ^{13}C NMR. These esters were then dissolved in a small volume of neat TFA (10 mL) and the reaction was allowed to proceed for 24 h at room temperature. Excess TFA was evaporated and the free carboxylic acids were precipitated in ethyl ether as white solids and their structures were also confirmed by ^{1}H and ^{13}C NMR. Spectroscopic data for the four peptide ligands and their *tert*-butyl ester precursors are supplied as supporting information.

2.2.2. Peptide-chitosan (PC) derivatives

Chitosan (0.9 g, 4.4 mmol of free $-NH_2$) was added portion-wise, over 1 h, to an aqueous solution (20 mL) containing four molar equivalents of the N^{α}-(3-bromopropanoyl)-amino acid ligand, as previously described (Batista et al., 2006; Scheme 2). When necessary, the insoluble fraction was separated by filtration. An equivalent amount of $NaHCO_3$ was added portion-wise to the chitosan/peptide solution, which was stirred for additional 30 min to remove the excess of CO_2 (pH 6.5). After stirring at 60 °C for 6 h, $NaHCO_3$ (1 g) was added (pH 8.5) and stirring was continued until the reaction was seen to have no further evolution (constant pH). Polymer precipitation with ethanol was done to separate the polymeric product from the excess of low-molecular-weight reactants. The precipitate was filtered and dissolved in water, acidified to pH 1–2 with concentrated HCl, dialyzed against deionized water over 2–3 days (Spectra/Por dialysis tube membrane, M_W cut-off 1 kDa, No. 132638) and freeze-dried (Christ alpha 1–4 freeze-drier) prior to further studies, detailed below.

2.2.3. Infrared spectroscopy (FTIR)

FTIR spectra of KBr pellets of chitosan and PC derivatives were recorded on a Jasco FT/IR-460 instrument. All spectra were acquired from 32 scans between 4000 and 400 cm^{-1} at a resolution of 4 cm^{-1} and were run in duplicate.

2.2.4. Nuclear magnetic resonance (NMR)

NMR spectra were recorded on a Bruker AMX 300 spectrometer. Peptide ligands and their ester precursors were dissolved in DMSO-d_6 and $CDCl_3$, respectively, to which tetramethylsilane (TMS) was added as internal reference. Chitosan was dissolved in DCl/D_2O 1:100 (v/v) and the PC derivatives in DCl/D_2O 1:1 (v/v), and 3-(trimethylsilyl)-1-propanesulfonic acid (DSS) was added to all polymer solutions as internal standard for ^{1}H NMR chemical shifts. The ^{1}H NMR spectra of the polymers were recorded at 70 °C for signal resolution improvement.

2.2.5. Potentiometric titrations (PT)

All titrations were performed in duplicate in the 2–10 pH range, with a high precision titration system and the same general conditions previously described (Skorik et al., 2003, 2005). A solution of each sample of the PC derivatives (~1.7 mmol L^{-1} of amino groups), arbitrarily represented as Glc-HNR, was prepared by dissolving a prescribed amount of the polymer with a known volume of 0.1000 mol L^{-1} HNO_3 necessary to achieve complete protonation of the PC polymers. After ionic strength adjustment with 0.1 mol L^{-1} KNO_3, the titration was conducted with a carbonate-free (Albert & Sergeant, 1971) 0.1 mol L^{-1} KOH standardized just before each titration. The glass electrode was calibrated in terms of hydrogen ion concentration by using buffers in the pH range 4–9 with ionic strengths adjusted to 0.1 with KNO_3 (Vasconcelos & Machado, 1986). The acid-base parameters were calculated and refined

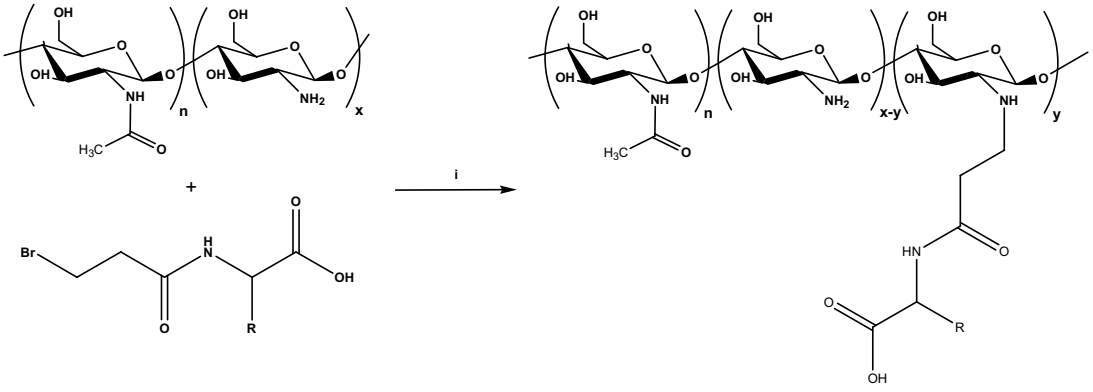

Scheme 2. Synthesis of the peptide-chitosans, (i) $NaHCO_3$(aq.), $T = 60$ °C; R = amino acid side chain.

with the HYPERQUAD program (Gans, Sabatini, & Vacca, 1996).

2.2.6. Differential scanning calorimetry (DSC)

The thermal behavior of chitosan and PC derivatives was determined by DSC. The samples were stored for 72 h under low humidity conditions, *i.e.*, on a vacuum desiccator over silica-gel, prior to thermal analysis. A NETZSCH – DSC 204 calorimeter, equipped with a controlled TASC 414/3A were used. Samples (1–2 mg; Mettler M3 Microbalance) were scanned in crimped sealed aluminium pans under nitrogen atmosphere (20 mL min^{-1}). An empty pan was used as reference. The temperature interval used was 30–500 °C scanned at 10 °C/min.

2.2.7. Scanning electron microscopy (SEM)

The surface morphologies of chitosan (CT), freeze-dried chitosan (FdCT) and peptide chitosan (PC) derivatives were examined by SEM. The samples were sputtered-coated with gold (10–20 nm thick; JEOL JFC 1100) and observed using a JEOL JSM-6301F scanning electron microscope.

3. Results

3.1. Infrared spectroscopy

FTIR was employed to examine the structural changes caused by insertion of peptide ligands into the parent chitosan polymer. The IR spectrum of chitosan is characterized by: large and intense bands at 3450–3200 cm^{-1} (hydrogen-bonded O–H stretching overlapped with the several N–H stretching bands); C–H stretching at 2783 cm^{-1}; bands due to the GlcNHAc units, with amide I (C═O stretching) at 1650 cm^{-1}, amide II (N–H bending) at 1565 cm^{-1}, amide III (C–N stretching coupled with N–H plane deformation) at 1412 cm^{-1} and symmetrical angular deformation of $–CH_3$ at 1376 cm^{-1}; C–N stretching of the amino groups at 1325 cm^{-1}; O–H plane deformation at 1262 cm^{-1}; C–O–C stretching vibration in the glucopyranose ring at 1028 cm^{-1}; and the specific bands of the $\beta(1 \rightarrow 4)$ glycoside bridge at 1153 and 895 cm^{-1} (Mansouri et al., 2004; Tian, Liu, Hu, & Zhao, 2004).

In comparison with the chitosan FTIR spectrum, *N*-(γ-propanoyl-glycine)-chitosan and *N*-(γ-propanoyl-phenylalanine)-chitosan spectra showed new absorption peaks at 1738 and 1736 cm^{-1}, respectively (Fig. 1, encircled peaks), corresponding to the C═O stretching mode of the carboxyl-functionalized ligands. These bands were also present in the FTIR spectra of the peptide-chitosans previously reported and unmistakably confirm the insertion of the peptide ligands (Batista et al., 2006). The analysis of the amide I, amide II and amide III regions is not straightforward for the PCs; bands due to the amide of GlcNHAc will be overlapped to those due to the amide bond from the peptide ligand and, further, to bands arising from ionized groups, namely, $–COO^-$ stretching and

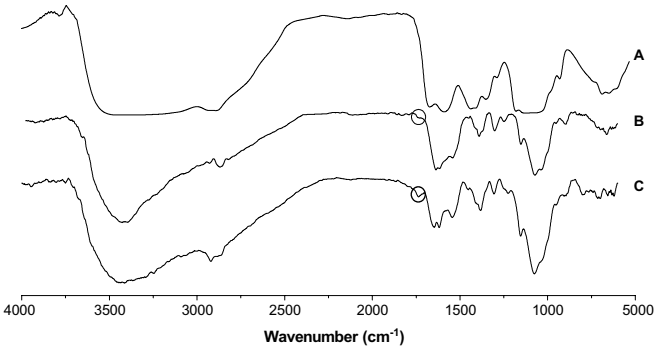

Fig. 1. FTIR spectra (KBr pellets) of (A) Chitosan; (B) *N*-(γ-propanoyl-glycine)-chitosan and (C) *N*-(γ-propanoyl-phenylalanine)-chitosan.

$–NH_3^+$ bending (Lin et al., 2005), turning unequivocal band attribution in this region a virtually impossible task. Nonetheless, as PC polymer's DA (∼10%) are smaller than their degree of substitution (DS), as determined by ^1H NMR (*cf* Section 3.2), spectral characteristics in the amide I–amide III region will be mainly determined by the peptide ligand rather than by the GluNHAc units. Thus, differences are to be expected in this region when comparing FTIR spectra of the PC with the spectrum of unmodified chitosan. In fact, a clear shift of transmittance minima to lower wavenumbers in the amide I, II and III regions (Liu, Du, Yang, & Zhu, 2004; Peniche et al., 1999) is observed for both *N*-(γ-propanoyl-glycine)-chitosan and *N*-(γ-propanoyl-phenylalanine)-chitosan, respectively, as follows: amide I, 1620 and 1616 cm^{-1}; amide II, 1546 and 1544 cm^{-1}; amide III, 1395 and 1383 cm^{-1}. This, again, shows that peptide ligands were inserted into the chitosan matrix.

3.2. ^1H NMR spectroscopy

Chemical structure of the PC polymers was determined by ^1H NMR spectroscopy. The ^1H NMR spectra of the modified chitosans are displayed in Fig. 2A (*N*-(γ-propanoyl-glycine)-chitosan) and B (*N*-(γ-propanoyl-phenylalanine)-chitosan) and the corresponding spectral data are given below. Fig. 2A shows signals at 4.56, 4.80 and 4.92 that were assigned to the H-1 hydrogen from acetylated, unsubstituted and monosubstituted units of D-glucosamine, respectively. Similarly, Fig. 2B shows overlapping signals from 4.99 to 5.19 that were assigned to the H-1 hydrogen from acetylated, unsubstituted and monosubstituted D-glucosamine units. An identical pattern was previously noted in our work on *N*-(γ-propanoyl-valin)-chitosan and *N*-(γ-propanoyl-aspartic acid)-chitosan (Batista et al., 2006). These results confirm the effective insertion of the peptide ligands in the chitosan biopolymer, corroborating the FTIR analysis above discussed.

Peaks attributed to reducing end protons of H-1 (Ishiguro, Yoshie, Sakurai, & Inoue, 1992) were observed at 5.14 and 5.34 ppm for (*N*-(γ-propanoyl-glycine)-chitosan) and

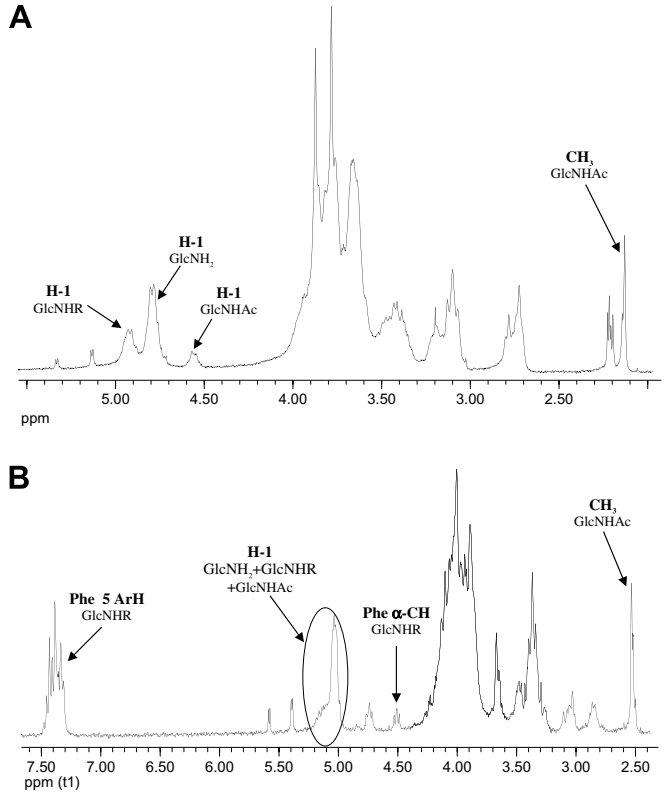

Fig. 2. ^{1}H NMR spectra (D_2O/DCl 1:1 v/v, 70 °C, 300 MHz) of (A) *N*-(γ-propanoyl-glycine)-chitosan and (B) *N*-(γ-propanoyl-phenylalanine)-chitosan.

at 5.40 and 5.59 ppm for (*N*-(γ-propanoyl-phenylalanine)-chitosan), suggesting that some degree of polymer hydrolysis occurred in the course of the NMR experiments. This interpretation is supported by a previous work from Vårum et al., who thoroughly studied the acid hydrolysis of chitosans by evaluating the influence of several factors on the rate and selectivity of hydrolysis of chitosans in the presence of hydrochloric acid (Vårum, Ottøy, & Smidsrød, 2001). These authors observed that the rate of de-*N*-acetylation was similar to the rate of hydrolysis of the glycosidic linkage in dilute acid, whereas the glycosidic linkages hydrolyzed *ca.* 10 times faster than de-*N*-acetylation in concentrated HCl (12.08 M). Also, different hydrolysis rates were measured for the four different glycosidic linkages, A–A, A–D, D–A and D–D, where A stands for a GlcNHAc and D for a $GlcNH_2$ unit. The first two types hydrolyzed at virtually the same rate but at about three times faster than the latter two. Finally, hydrolysis rates markedly increased with HCl concentration, time, temperature and polymer's DA. Overall, the findings from Vårum et al. (Vårum et al., 2001) explain our observations, as our samples were dissolved in DCl at ~6 M in D_2O and spectra were acquired at high temperature (70 °C) over extended periods of time ($\geqslant$6 h). Polymer hydrolysis could be minimized by running the NMR experiments at lower DCl concentration, lower temperature and/or shorter acquisition times, but attempts to run the NMR experiments in such a way failed to yield spectra with adequate quality (poor signal resolution and/or overlapping of relevant peaks with the D_2O signal were observed).

NMR peak integrals allowed us to determine the DA and DS for each PC polymer. Taking χ as the sum of the integrals measured for peaks of H-1 from GlcNHAc, $GlcNH_2$ and GlcNHR units in each polymer (Fig. 2), DA was calculated as the quotient between 1/3 the integral of the $-CH_3$ peak at 2.13 ppm (Fig. 2A) or 2.50 ppm (Fig. 2B) and the value of χ for the corresponding polymer. DA was found to be ~10% for both polymers, matching the value of the commercial chitosan used. Therefore, reaction conditions for the insertion of the peptide ligands were mild enough to keep the polymer's DA unchanged, as expected. The DS value for *N*-(γ-propanoyl-glycine)-chitosan was calculated as the quotient between the integral measured for the peak of H-1 from GlcNHR (4.92 ppm, Fig. 2A) and the χ sum obtained for this polymer. However, in the case of *N*-(γ-propanoyl-phenylalanine)-chitosan, the peak of H-1 from GlcNHR was not resolved, so the integral of the phenylalanine α-CH proton or 1/5 the integral of the phenylalanine aromatic protons (Fig. 2B) were used instead. DS values of 26% and 12% were thus obtained for *N*-(γ-propanoyl-glycine)-chitosan and *N*-(γ-propanoyl-phenylalanine)-chitosan, respectively, the first one comparing well with the DS values of 32% and 27% previously found for *N*-(γ-propanoyl-valin)-chitosan and *N*-(γ-propanoyl-aspartic acid)-chitosan, respectively (Batista et al., 2006). However, the DS value for the phenylalanine-based polymer (12%) is significantly lower than those for the other three PC polymers (averaged to 28%). This can be attributed to a combination of two factors, namely, (i) the observed low solubility of N^{α}-(3-bromopropanoyl)-phenylalanine in the aqueous reaction medium, and (ii) influence of the bulky amino acid side chain (benzyl group) on reactivity. However, the point at which the four α-amino acids differ from each other (*i.e.*, their side chains) is five bonds apart from the terminal bromo-methylene group where the S_N2 occurs, so the amino acid side chain is expected to have only little influence on reactivity. Thus, solubility problems seem to be the main cause for the low DS obtained for *N*-(γ-propanoyl-phenylalanine)-chitosan. Not taking into account this particular case, we may say that, under the conditions employed, the average yield for the insertion of N^{α}-(3-bromopropanoyl)-amino acid ligands into the chitosan polymeric chain is of ~30%.

3.2.1. *N*-(γ-Propanoyl-glycine)-chitosan (Fig. 2A)

δ_H/ppm (D_2O/DCl 1:1 v/v, 70 °C, 300 MHz): 2.13–2.23 (m, 0.33 H, $-\boldsymbol{CH}_3$ of GlcNHAc from polymer + hydrolyzed units), 2.76 (m, 0.52H, $-CH_2C\boldsymbol{H}_2CONH-$ from GlcNHR), 3.13 (m, 0.95H, ***H-2*** from GlcNHR and $GlcNH_2$), 3.35–4.10 (m, 6.01H, ***H-2*** from GlcNHAc, $-C\boldsymbol{H}_2CH_2CONHC\boldsymbol{H}_2COOH$ from GlcNHR and H-3,4,5, 6a and 6b from $GlcNH_2$, GlcNHR and GlcNHAc), 4.56 (d, 0.10H, ***H-1*** of GlcNHAc), 4.80 (d, 0.60H, ***H-1*** from $GlcNH_2$), 4.92 (d, 0.24H, ***H-1*** from GlcNHR), 5.14 (d,

0.14H, ***H-1*** from $GlcNH_2$, hydrolyzed unit), 5.34 (d, 0.02H, ***H-1*** from GlcNHR, hydrolyzed unit).

3.2.2. N-(γ-Propanoyl-phenylalanine)-chitosan (Fig. 2B)

δ_H/ppm (D_2O/DCl 1:1 v/v, 70 °C, 300 MHz): 2.52 (m, 0.30H, –***CH***$_3$ from GlcNHAc), 2.85 (m, 0.25H, –CH_2C***H***$_2$CONH– from GlcNHR), 3.06 (m, 0.25H, –C***H***$_2$Ph from GlcNHR), 3.37–4.30 (m, 6.02H, ***H-2*** from GlcNHR and $GlcNH_2$, –C***H***$_2CH_2$CONH– from GlcNHR and H-3,4,5,6, from $GlcNH_2$, GlcNHR and GlcNHAc), 4.51 (t, 0,12H,–C***H***CH_2Ph), 4.74 (t, 0.10H, ***H-2*** from GlcNHAc), 4.99–5.19 (m, 0.83H, ***H-1*** from GlcNHAc, $GlcNH_2$ and GlcNHR), 5.40 (d, 0.12H, ***H-1*** from $GlcNH_2$ hydrolyzed unit), 5.59 (d, 0.05H from GlcNHR hydrolyzed unit), 7.39 (m, 0.62H, ***H*** phenyl group of GlcNHR).

Finally, the knowledge of the DS values of all PC polymers, as deduced from ^{1}H NMR data, provides a means to estimate the M_Ws of the four polymers. The commercial chitosan used has a M_W of 150 kDa and DA=10%, which means that it is composed by 90% $GlcNH_2$ units (M_W = 161.16 Da) and 10% GlcNHAc units (M_W = 203.19 Da). Thus, the parent polymer combines ~819 $GlcNH_2$ monomers with ~91 GlcNHAc units. The PCs prepared have a percentage of the 819 $GlcNH_2$ units equal to the polymer's DS where the $–NH_2$ groups are replaced by the corresponding –NHR. Simple calculations, using the polymers' DS values and the M_Ws of the different R ligands, allow us to estimate the following M_Ws for the PC polymers: *N*-(γ-propanoyl-glycine)-chitosan, ~185 kDa; *N*-(γ-propanoyl-phenylalanine)-chitosan, ~176 kDa; *N*-(γ-propanoyl-valin)-chitosan, ~205 kDa; *N*-(γ-propanoyl-aspartic acid)-chitosan, ~201 kDa. As expected, peptide ligand insertion increased the global M_W of the polymers, as compared to unmodified chitosan, by 17–34%. These increments reflect both the M_W of the peptide ligands and the DS attained under the reaction conditions employed. Therefore, higher M_W increments should be expected for longer reaction times or greater molar excesses of the peptide ligand, as a consequence of the higher DS that would be theoretically reached. However, we have observed that, using four molar equivalents of the peptide ligand, the reaction did not further progress after 6 h, so longer reaction times would hardly lead to increased DS. Thus, higher M_Ws would most probably be reached only by increasing the molar excess of the peptide ligand used in the reaction, as harsher reaction conditions should be avoided. Anyway, a maximum ligand insertion level would most probably be reached, so much greater increments of final polymer's M_W are probably difficult to attain.

3.3. Potentiometric studies

Potentiometric titrations of fully protonated PC and CT polymers were carried out by addition of carbonate-free KOH solution to the polymer aqueous solutions. All PC polymers were completely soluble in the 2–10 pH range, as visually checked in the course of the titrations. Even though visual inspection may be considered as not enough accurate to be used as a tool for solubility evaluation, the fact is that, in the course of identical potentiometric titrations on unmodified chitosan solutions, turbidity is observed when the pH is reaching 6 and, when pH reaches 6.5, polymer precipitation starts to occur. None of these phenomena were seen for the PC polymers, and that is enough prove that, at the macroscopic level, peptide-chitosans are significantly more water-soluble than the parent chitosan over the entire pH range used in the titrations. This is even more remarkable if we take into account that the new PC polymers have slightly higher M_W (averaged to ~192 kDa) than the parent chitosan (~150 kDa), as higher M_Ws would contribute to a decreased solubility in aqueous media.

In order to accurately determine the acidity constants of the polymers, three models were taken into account: *Model 1* – The polymer was considered as a diprotic species, whose concentration is the same of the ionisable amino groups. *Model 2* – Amino and carboxylic groups were treated as two independent monoprotic species and the concentration of the carboxylic groups considers the DS. *Model 3* – Same as *Model 2*, but the amino groups were separated into primary and secondary amino groups and treated as two independent monoprotic species. Together with the carboxylic groups, they compose a system with three monoprotic species. The results obtained by fitting the experimental data to each of the three models allowed us to conclude that the best fits (Hyperquad σ statistical parameter – Fig. 3) were obtained with *Model 3*, suggesting that this model describes a more realistic picture of the ongoing acid-base phenomena. Indeed, curve-fitting with *Model 3* yielded two distinct pK_a values related to basic groups (Table 1), which reflects the presence of primary and secondary amines, as the latter usually have higher pK_a values than the former. Table 1 shows that pK_1^H values

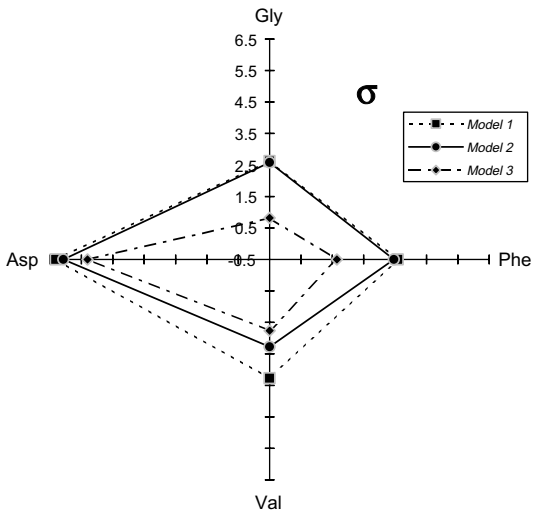

Fig. 3. Statistical parameter, σ, for the refinement (Hyperquad) of PC titration curves using *Models 1–3* to describe the acid-base system.

Table 1
pK_a values obtained by fitting experimental data to *Model 3*

Polymers	PESH		
	$-\log K_1^H$	$-\log K_2^H$	$-\log K_3^H$
Chitosan	6.40 ± 0.01	–	–
N-(γ-Propanoyl-glycine)-chitosan	6.08 ± 0.01	7.42 ± 0.03	3.03 ± 0.04
N-(γ-Propanoyl-phenylalanine)-chitosan	6.12 ± 0.01	7.68 ± 0.07	2.7 ± 0.1
N-(γ-Propanoyl-valine)-chitosan	6.13 ± 0.04	7.26 ± 0.08	3.68 ± 0.05
N-(γ-Propanoyl-aspartic acid)-chitosan	5.80 ± 0.01	7.2 ± 0.2	2.3 ± 0.2

for the PC polymers vary in the 5.80–6.13 range and compare well with the pK_1^H value for chitosan (6.40) that has only primary amino groups. Moreover, the PC's pK_2^H values, attributed to the ionization of the secondary amines, vary in the 7.2–7.68 range, thus being higher than the corresponding pK_1^H, as expected. The distinctive acid-base properties displayed by chitosan and the four PC polymers constitute an additional indirect proof of successful peptide ligand insertion into the polymer matrix and provide a means for the fine-tuning of pH-related properties of these new materials. Again, the most obvious advantage of our PC polymers is their solubility in aqueous medium over a wide pH-range (at least, from pH 2 to pH 10), in clear contrast with chitosan that is only highly soluble in acidic media ($pH \leqslant 6$).

3.4. Differential scanning calorimetry

DSC thermograms of chitin (CH), CT and FdCT (Fig. 4A–C) exhibit an endothermic peak around 73, 100 and 87.3 °C, respectively, attributed to the thermal evaporation of bound water that could not be removed completely upon drying (Elizabeth & Pillai, 2006), which constitutes the polymer's water holding capacity (WHC) (Kittur, Prashanth, Sankar, & Tharanathan, 2002; Prashanth, Kittur, & Tharanathan, 2002; Rueda, Secall, & Bayer, 1999; Tirkistani, 1998). Water is essentially bound through the –OH and free $–NH_2$ hydrophilic groups of chitosan (Sato et al., 1997). The endothermic peak of FdCT presents a shift towards a lower temperature relatively to CT. This can be explained considering that the process of solubilization followed by freeze-drying of chitosan alters its supramolecular structure, simplifying the polymer's hydrogen bond network. The endothermic peak of CH appears at the lowest temperature, as water is essentially adsorbed to the CH surface. The endothermic peak areas follow the order FdCT ($\Delta H = 648.4$ J/g) > CT ($\Delta H = 322.7$ J/g) > CH ($\Delta H = 171.58$ J/g), reinforcing the existence of a correlation between the chemical and supramolecular structure of the polymers and their WHC (Kittur et al., 2002). So, these differences can again be explained by the fact that FdCT can have additional free –OH and $–NH_2$ groups, previously engaged in inter-chain hydrogen bonds, available for hydrogen-bonding to more water molecules. Further, FdCT is not as compact as CT, thus its increased area can hold more surface-adsorbed water.

The second thermal event is an exothermic peak at 397, 307 and 292 °C, respectively, for CH, CT and FdCT, and can be attributed to the thermal degradation of these polymers (Qin et al., 2003). The exothermic peaks of CH, CT and FdCT also present a progressive shift towards lower temperatures, which can also be explained by a progressive weakening of the polymer supramolecular structure that becomes increasingly thermo-sensitive.

In the case of the peptide-chitosan polymers (Fig. 5A–D), the endothermic peaks were displaced to lower temperatures relatively to CT, appearing between 77 and 90 °C. The same behavior was observed for the exothermic peaks,

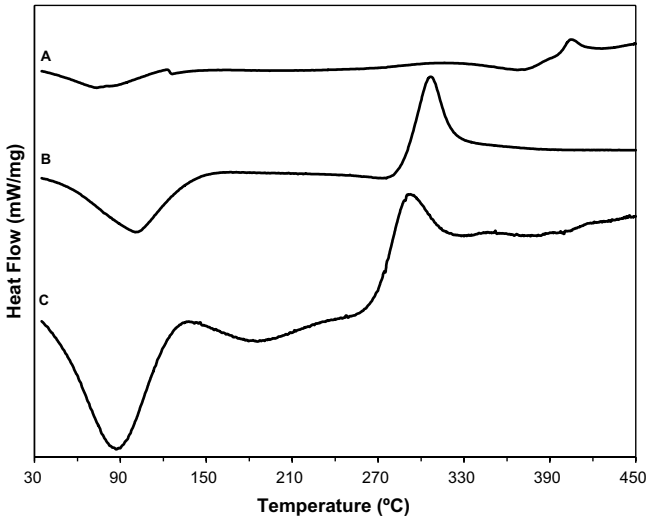

Fig. 4. DSC thermograms of (A) chitin, (B) chitosan, (C) freeze-dried chitosan.

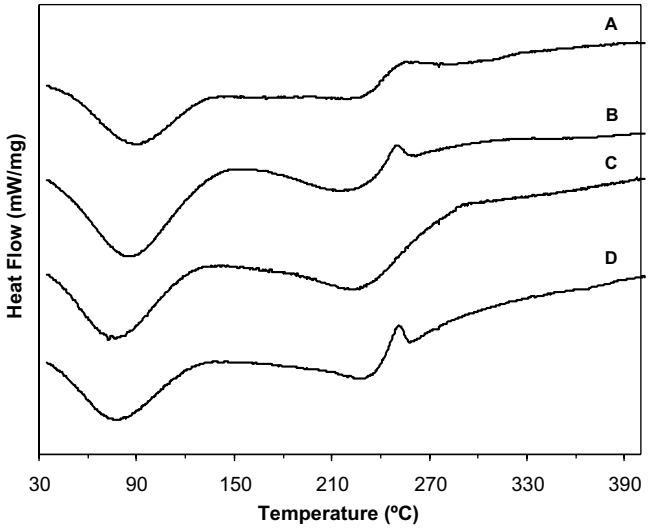

Fig. 5. DSC thermograms of (A) *N*-(γ-propanoyl-valin)-chitosan, (B) *N*-(γ-propanoyl-aspartic acid)-chitosan, (C) *N*-(γ-propanoyl-glycine)-chitosan and (D) *N*-(γ-propanoyl-phenylalanine)-chitosan.

spanning wider amplitude of temperatures: 217–252 °C. This downward shift of both the endothermic and exothermic peaks indicates that a significant change in the chemical and supramolecular structure of chitosan occurs when additional functional groups are grafted onto the polymeric matrix. The peptide ligands thus seem to increase the polymer's WHC through the insertion of additional amide and carboxyl groups.

Based on the area of the endothermic peaks, we found that B ($\Delta H = 389.6$ J/g) > C ($\Delta H = 273.6$ J/g) > D ($\Delta H = 248.0$ J/g) > A ($\Delta H = 218.9$ J/g) (Fig. 5), following the decrease in hydrophilic character of the ligand –R (Scheme 2), which can be associated with a relative decrease in the polymer's WHC. Insertion of the Asp-based ligand into the polymer matrix (curve B) induces a much more dramatic effect on ΔH values for the endothermic transition than do the ligands based on the other three amino acids. This can be ascribed to the fact that Asp was the only tri-functional amino acid used, *i.e.*, the only one with a functional group in its side chain, namely, a carboxyl group. The presence of two carboxyl groups in the Asp-based ligand has two implications: (i) this ligand is much more hydrophilic than the other three, and (ii) repulsion between carboxylates weakens the polymer supramolecular structure to a much higher extent. As to the temperatures at which the endothermic event happens, these follow the order A ($T_{max} = 90.8$ °C) > B ($T_{max} = 85.9$ °C) > D ($T_{max} = 79.0$ °C) > C ($T_{max} = 76.8$ °C). So, there seems to be no obvious correlation between the temperature of the endothermic transition with either ligand size or hydrophilic character.

Looking at the exothermic peaks on the thermograms of the PC polymers, three of them degraded at lower temperatures than FdCT, but a marked exothermic peak was not observable for the glycine-based polymer (curve C), and an accurate determination of thermo-degradation parameters for this PC was not possible. The thermo-degradation temperatures are similar between the other three PC, but the polymer's thermo-sensitivity seems to be correlated with the ligand's hydrophilic character: A ($T_{max} = 255.0$ °C) > D ($T_{max} = 252.5$ °C) > B ($T_{max} = 250.0$ °C). Consequently, a significant perturbation of the naturally strong and ordered structure of chitosan is caused by insertion of the peptide ligands, yielding more thermo-sensitive derivatives whose stability seems to decrease with the increasing hydrophilic character of the ligand. Again, we think that the two carboxyl groups from the Asp-based ligand contribute to the weakening of the polymeric structure both due to a higher capacity to bind water and to a stronger repulsion between the negatively-charged carboxylates. Our results agree with observations from other authors (Elizabeth & Pillai, 2006; Gocho, Shimizu, Tanioka, Chou, & Nakajima, 2000; Kittur et al., 2002; Sarmento, Ferreira, Veiga, & Ribeiro, 2006), reinforcing that grafting of hydrophobic or hydrophilic ligands to chitosan results in a decrease of polymer crystallinity by: (i) loosening the intra- and inter-chain hydrogen bonds that characterize the rigid polymer matrix, and (ii) increasing the number of free hydroxyl and amino groups available to bind water molecules. This leads to increased WHC and thermo-sensitivity, as observed in our case for the PC polymers. The second event on the thermograms of our PC polymers can also be interpreted according to what has been suggested by Kittur et al. (2002) and Sarmento et al. (2006), who considered this event as the association of two peaks: a smaller endothermic peak corresponding to the loss of crystallization water strongly bound to the closely-packed polymeric structure, immediately followed by a larger exothermic peak due to polymer-degradation, *i.e.*, de-polymerization and degradation of side chains and substituents (Britto & Campana-Filho, 2004). In our case, the second event can also be seen as a superposition of two peaks, which becomes clearer for PC polymers (Fig. 5B and D).

3.5. Scanning electron microscopy

SEM micrographs show that the freeze-drying process causes a significant change in the chitosan structure (Fig. 6A and B). Commercial chitosan (CT, Fig. 6A) is a powder that shows a compact morphology under the SEM, whereas, after freeze-drying (FdCT, Fig. 6B), it adopts a stripped film-like aspect. The morphology of FdCT is similar to those presented by the peptide derivatives (Fig. 6C–F). However, these have a more irregular, sponge-like, surface, especially in the cases of *N*-(γ-propanoyl-aspartic acid)-chitosan (Fig. 6D and insert) and *N*-(γ-propanoyl-phenylalanine)-chitosan (Fig. 6F and insert). Once again, and in agreement with our observations in DSC experiments, both freeze-drying and peptide ligand-insertion lead to de-compacting of the polymeric matrices and, in the case of PC polymers, to some quite surprising morphologies that resemble either bone-like or honeycomb-like structures. These highly porous structures may become particularly interesting for potential biomedical applications of these PC polymers.

4. Discussion

Chitosan is a non-toxic and soft-tissue compatible polymer with a special ability to adhere to mucosal surfaces and to transiently open the junctions between epithelial cells (Artursson, Lindmark, Davis, & Illum, 1994; Kotzé et al., 1999). There are several potential biomedical applications for low molecular weight chitosans, but many of them are limited by the polymer's low solubility above pH ~ 6. Effectively, chitosan is soluble in the stomach acidic conditions but precipitates in the intestinal tract, so it is only residually absorbed in the intestine. This characteristic has been exploited for the development of chitosan-based "fat-trappers" as weight reducers: in the stomach, fat is emulsified by dissolved chitosan, after which the chitosan-fat emulsion precipitates upon arrival to the intestine, from which it is excreted. Still, the limited

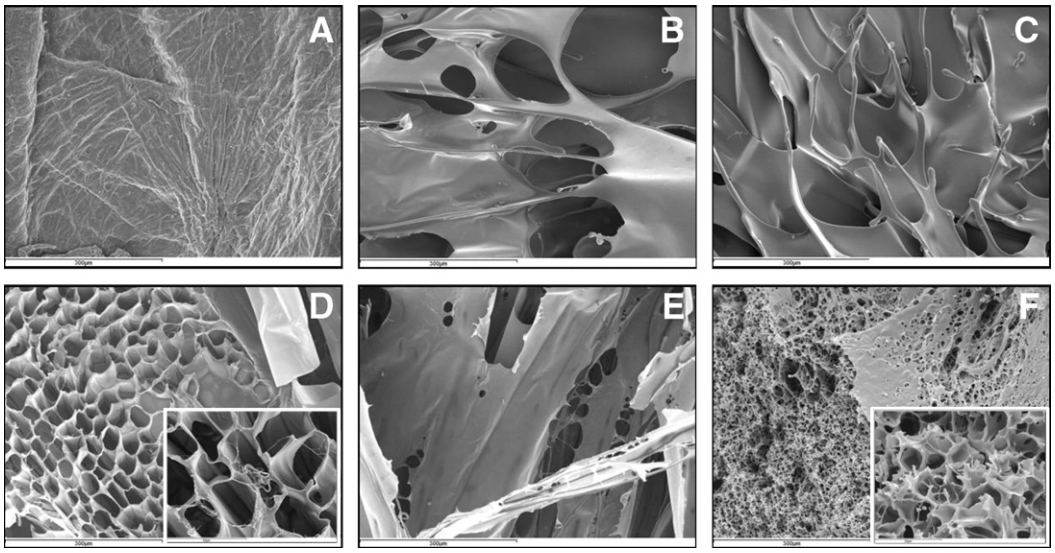

Fig. 6. SEM photographs (200× magnification) of (A) chitosan (CT), (B) lyophilised chitosan (FdCT), (C) *N*-(γ-propanoyl-valin)-chitosan, (D) *N*-(γ-propanoyl-aspartic acid)-chitosan (insert: 1000× magnification), (E) *N*-(γ-propanoyl-glycine)-chitosan and (F) *N*-(γ-propanoyl-phenylalanine)-chitosan (insert: 2500× magnification).

solubility of chitosan makes it unsuitable for many therapeutic applications. Having the purpose of overcoming this obstacle, we have successfully prepared chitosan derivatives through covalent binding, to the polymer's amino groups, of peptide ligands obtained by condensation of 3-bromopropanoic acid with natural α-amino acids. These new polymers possess positively (primary amino) and negatively (carboxyl) charged groups and are fully water-soluble in the physiological pH range. This is a major advantage for chitosan-based vehicles for oral drug administration as, for instance, Thanou et al. have found that *N*-trimethylchitosan chloride is water-soluble in the entire pH range and acts as an absorption enhancer for oral peptide drug delivery by facilitating the paracellular peptide transport (Thanou, Florea, Langemeÿer, Verhoef, & Junginger, 2000; Thanou, Verhoef, Marbach, & Junginger, 2000; Thanou, Verhoef, Verheijden, & Junginger, 2001; Thanou et al., 1999; Van der Merwe et al., 2004). Other examples, where combination of opposite charges combined in chitosan-based materials leads to interesting drug delivery properties, have been described by Tapia et al. (2004), who reported chitosan-alginate complexes as prolonged drug release systems, by Thierry et al. (2005), who developed a polyelectrolyte multilayered platform for the administration of paclitaxel, and by Ruel-Gariépy et al. (2004), who showed that a thermo-sensitive chitosan/β-glycerophosphate hydrogel may have an important role for the local delivery of paclitaxel. Also, Lin et al. (2005) reported chitosan and poly-γ-glutamic acid co-polymeric nanoparticles with enhanced intestinal paracellular transport properties. This enhancement can be attributed to the carboxylates from the poly-γ-glutamic acid, as they partially cancel the cationic character of chitosan, yielding a more zwitterionic material, thus with extended water-solubility over a wider pH range. In view of all this, it is reasonable to expect that our new peptide-chitosans can act as enhancers for oral drug absorption through the paracellular pathway, and such will be perhaps more pronounced for the Asp-derived polymer that has higher carboxylate content. Further, our peptide-chitosans are expected to be more stable under physiological conditions than the above mentioned co-polymers, as the anionic portion in our case is covalently attached to chitosan.

Variation of reaction time and/or stoichiometry in ligand insertion can be used to produce different degrees of substitution, *i.e.* different NH_3^+/COO^- ratios, according to specific needs for each particular case. The ammonium groups are important for electrostatic immobilization of anionic drugs and account for the bioadhesive, bacteriostatic and blood cell affinity properties of chitosan-based hydrogels (Amaral et al., 2005; Liao, Lin, & Wu, 2005). On the other hand, the presence of carboxyl groups in the same polymer not only provides a means for the electrostatic immobilization of cationic drugs, but also promotes a reversible and pH-dependent ionic cross-linking of the matrix that is desirable over irreversible covalent cross-linking of hydrogels for biomedical applications (Berger et al., 2004).

The insertion of carboxyl groups into the chitosan matrix has also the important advantage of providing an additional functionality that can be used for different purposes. Thus, these peptide-chitosans offer the possibility of making use of alcohol, amine and carboxylic acid chemistries either for drug covalent immobilization or for additional modifications to modulate the polymer's properties. For instance, we can picture the covalent immobilization an aminated drug by condensation of its amino group to the carboxylated chain of the polymer, yielding an enzyme-labile amide bond. This can be easily achieved through peptide coupling chemistry similar to that described for covalent binding of the *C*-terminal carboxyl group of bioactive peptides to the chitosan's amino

groups (Hojo et al., 1999). Such polymer-drug conjugate can work as a system for drug transport and delivery *in vivo* that potentially: (i) protects the drug from metabolic inactivation, (ii) protects the patient from the drug's secondary effects and (iii) allows for controlled drug release through enzymatic hydrolysis of the drug–polymer amide bond. Since this bond involves both the drug and a proteinogenic α-amino acid from the PC polymer, it is highly probable that it is recognized by proteases. On the other hand, as enzymes have to reach the sites within the polymer matrix at which the drug is attached, release will most probably be slow. This is a picture that can be drawn for virtually any drug that can be attached to our peptide-chitosans through enzyme-labile bonds, given that the polymers are ''water-friendly'' and porous enough to allow the enzyme to enter and play its role. The new peptide-chitosans herein reported also have the right properties to ensure this, as they are significantly less ordered and more porous than the parent chitosan, as shown by the thermotropic (DSC) and morphological (SEM) studies carried out. This higher disorder leads to the higher surface area and water-holding capacity that characterizes these materials, more pronouncedly in the case of the Asp-derived polymer, and will probably have a key role in their performance as biocompatible and biodegradable hydrogels for drug transport and controlled release *in vivo*.

5. Conclusion

Our main objective was to surpass the obstacles related to chitosan's limited solubility. With this goal in mind, we have successfully prepared carboxylated chitosan derivatives through covalent binding of *N*-(3-bromopropanoyl)-amino acid (peptide) ligands to the polymer's primary amino groups. The new polymers were obtained with DS values around ~30%, except in the case of the Phe-derived polymer, and thus possess reduced net positive charge as compared to the parent chitosan. This provided the new peptide-chitosans with full water-solubility over practically the entire physiological pH range and led to more disordered and porous structures, with higher surface area and water-holding capacity. Globally, the new peptide-chitosans, and especially the Asp-derived polymer, possess physico-chemical properties that turn them into promising candidates as novel chitosan-based drug delivery systems.

Acknowledgments

The authors thank *FCT* for financial support to research units *CIQUP* (P.G.) and *LAQUIPAI* (C.G.) and also for Ph.D. Grant SFRH/BD/13144/2003 (M.B.). The authors are indebted to Dr. Yury A. Skorik (Department of Chemistry, Chevron Science Center, Pittsburgh, USA) for fruitful discussions.

References

Aiping, Z., Jianhong, L., & Wenhui, Y. (2006). Effective loading and controlled release of camptothecin by *O*-carboxymethylchitosan aggregates. *Carbohydrate Polymers, 63*, 89–96.

Albert, A., & Sergeant, E. P. (1971). *The determination of ionization constants*. London: Chapman and Hall.

Amaral, I. F., Lamghari, M., Sousa, S. R., Sampaio, P., & Barbosa, M. A. (2005). Rat bone marrow stromal cell osteogenic differentiation and fibronectin adsorption on chitosan membranes: The effect of the degree of acetylation. *Journal of Biomedical Materials Research, 75A*, 387–397.

Amaral, I. F., Sampaio, P., & Barbosa, M. A. (2005). Three-dimensional culture of human osteoblastic cells in chitosan sponges: The effect of the degree of acetylation. *Journal of Biomedical Materials Research, 76A*, 335–346.

Araújo, M. J., Bom, J., Capela, R., Casimiro, C., Chambel, P., Gomes, P., et al. (2005). Imidazolidin-4-one derivatives of primaquine as novel transmission-blocking antimalarials. *Journal of Medicinal Chemistry, 48*, 888–892.

Artursson, P., Lindmark, T., Davis, S. S., & Illum, L. (1994). Effect of chitosan on the permeability of monolayers of intestinal epithelial cells (Caco-2). *Pharmaceutical Research, 11*, 1358–1361.

Atyabi, F., Majzoob, S., Iman, M., Salehi, M., & Dorkoosh, F. (2005). In vitro evaluation and modification of pectinate gel beads containing trimethyl chitosan, as a multi-particulate system for delivery of water-soluble macromolecules to colon. *Carbohydrate Polymers, 61*, 39–51.

Batista, M. K. S., Pinto, L. F., Gomes, C. A. R., & Gomes, P. (2006). Novel highly soluble peptide-chitosan polymers: Synthesis and spectral characterization. *Carbohydrate Polymers, 64*, 299–305.

Berger, J., Reist, M., Mayer, J. M., Felt, O., & Gurny, R. (2004). Structure and interactions in chitosan hydrogels formed by complexation or aggregation for biomedical applications. *European Journal of Pharmaceutics and Biopharmaceutics, 57*, 35–52.

Berger, J., Reist, M., Mayer, J. M., Felt, O., Peppas, N. A., & Gurny, R. (2004). Structure and interactions in covalently and ionically cross-linked chitosan hydrogels for biomedical applications. *European Journal of Pharmaceutics and Biopharmaceutics, 57*, 19–34.

Bernkop-Schnürch, A. (2000). Chitosan and its derivatives: Potential excipients for peroral peptide delivery systems. *International Journal of Pharmaceutics, 194*, 1–13.

Bernkop-Schnürch, A., & Kast, C. E. (2001). Chemically modified chitosans as enzyme inhibitors. *Advanced Drug Delivery Reviews, 52*, 127–137.

Britto, D., & Campana-Filho, S. P. (2004). A kinetic study on the thermal degradation of *N*,*N*,*N*-trimethylchitosan. *Polymer Degradation and Stability, 84*, 353–361.

Chambel, P., Capela, R., Lopes, F., Iley, J., Morais, J., Gouveia, L., et al. (2006). Reactivity of imidazolidin-4-one derivatives of primaquine: implications for prodrug design. *Tetrahedron, 62*, 9883–9891.

Chandy, T., & Sharma, C. P. (1992). Chitosan beads and granules for oral sustained delivery of nifedipine: In vitro studies. *Biomaterials, 13*, 949–952.

Danielsen, S., Vårum, K. M., & Stokke, B. T. (2004). Structural analysis of chitosan mediated DNA condensation by AFM: Influence of chitosan molecular parameters. *Biomacromolecules, 5*, 928–936.

Delben, F., Gabrielli, P., Muzzarelli, R. A. A., & Stefancich, S. (1994). Interaction of soluble chitosans with dyes in water. II. Thermodynamic data. *Carbohydrate Polymers, 24*, 25–30.

Elizabeth, G., & Pillai, C. K. S. (2006). Chitosan/oligo L-lactide graft copolymers: Effect of hydrophobic side chains on the physico-chemical properties and biodegradability. *Carbohydrate Polymers, 64*, 254–266.

Gans, P., Sabatini, A., & Vacca, A. (1996). Investigation of equilibria in solution. Determination of equilibrium constants with the HYPERQUAD suite of programs. *Talanta, 43*, 1739–1753.

Gocho, H., Shimizu, H., Tanioka, A., Chou, T.-J., & Nakajima, T. (2000). Effect of polymer chain end on sorption isotherm of water by chitosan. *Carbohydrate Polymers, 41*, 87–90.

Gomes, P., Araújo, M. J., Rodrigues, M., Vale, N., Azevedo, Z., Iley, J., et al. (2004). Synthesis of imidazolidin-4-one and 1H-imidazo[2,1-a]isoindole-2,5(3H,9bH)-dione derivatives of primaquine: Scope and limitations. *Tetrahedron, 60*, 5551–5562.

Gupta, K. C., & Ravikumar, M. N. V. (2000). Drug release behavior of beads and microgranules of chitosan. *Biomaterials, 21*, 1115–1119.

Hojo, K., Maeda, M., Mu, Y., Kamada, H., Tsutsumi, Y., Nishiyama, Y., et al. (1999). Preparation of a chitosan hybrid of an antimetastatic laminin-related peptide. *Pharmacy and Pharmacology Communications, 5*, 277.

Holappa, J., Nevalainen, T., Savolainen, J., Soininen, P., Elomaa, M., Safin, R., et al. (2004). Synthesis and characterization of chitosan *N*-betainates having various degrees of substitution. *Macromolecules, 37*, 2784–2789.

Holappa, J., Nevalainen, T., Soininen, P., Elomaa, M., Safin, R., Másson, M., et al. (2005). *N*-chloroacyl-6-*O*-triphenylmethylchitosans: Useful intermediates for synthetic modifications of chitosan. *Biomacromolecules, 6*, 858.

Holappa, J., Nevalainen, T., Soininen, P., Másson, M., & Järvinen, T. (2006). Synthesis of novel quaternary chitosan derivatives via *N*-chloroacyl-6-*O*-triphenylmethylchitosans. *Biomacromolecules, 7*, 407–410.

Ishiguro, K., Yoshie, N., Sakurai, M., & Inoue, Y. (1992). A ^{1}H NMR study of a fragment of partially *N*-deacetylated chitin produced by lysozyme degradation. *Carbohydrate Research, 237*, 333–338.

Iwasaki, N., Yamane, S.-T., Majima, T., Kasahara, Y., Minami, A., Harada, K., et al. (2004). Feasibility of polysaccharide hybrid materials for scaffolds in cartilage tissue engineering: evaluation of chondrocyte adhesion to polyion complex fibres prepared from alginate and chitosan. *Biomacromolecules, 5*, 828–833.

Janes, K. A., Calvo, P., & Alonso, M. J. (2001). Polysaccharide colloidal particles as delivery systems for macromolecules. *Advanced Drug Delivery Reviews, 47*, 83–97.

Kittur, F. S., Prashanth, K. V. H., Sankar, K. U., & Tharanathan, R. N. (2002). Characterization of chitin, chitosan and their carboxymethyl derivatives by differential scanning calorimetry. *Carbohydrate Polymers, 49*, 185–193.

Kogan, G., Skorik, Y. A., Žitňanova, I., Križková, L., Ďuračková, Z., Gomes, C. A. R., et al. (2004). Antioxidant and antimutagenic activity of *N*-(2-carboxyethyl)chitosan. *Toxicology and Applied Pharmacology, 201*, 303–310.

Kotzé, A. F., Lueβen, H. L., Thanou, M. M., Verhoef, J. C., de Boer, A. G., Junginger, H. E., et al. (1999). Chitosan and chitosan derivatives as absorption enhancers for peptide drugs across mucosal epithelia. In E. Mathiowitz, D. E. Chickering, & C.-M. Lehr (Eds.), *Bioadhesive drug delivery systems: Fundamentals, novel approaches and development* (pp. 341–387). New York: Marcel Dekker.

Krauland, A. H., Guggi, D., & Bernkop-Schnürch, A. (2006). Thiolated chitosan microparticles: A vehicle for nasal peptide drug delivery. *International Journal of Pharmaceutics, 307*, 270–277.

Kurita, K., Ikeda, H., Yoshida, Y., Shimojoh, M., & Harata, M. (2002). Chemoselective protection of the amino groups of chitosan by controlled phthaloylation: Facile preparation of a precursor useful for chemical modifications. *Biomacromolecules, 3*, 1–4.

Liao, J.-D., Lin, S.-P., & Wu, Y.-T. (2005). Dual properties of the deacetylated sites in chitosan for molecular immobilization and biofunctional effects. *Biomacromolecules, 6*, 392–399.

Lin, Y.-H., Chung, C.-K., Chen, C.-T., Liang, H.-F., Chen, S.-C., & Sung, H. (2005). Preparation of nanoparticles composed of chitosan/poly-γ-glutamic acid and evaluation of their permeability through Caco-2 cells. *Biomacromolecules, 6*, 1104–1112.

Liu, H., Du, Y., Yang, J., & Zhu, H. (2004). Structural characterization and antimicrobial activity of chitosan/betaine derivative complex. *Carbohydrate Polymers, 55*, 291–297.

Liu, C. G., Desai, K. G. H., Chen, X., & Park, H. (2005). Linolenic acid-modified chitosan for formation of self-assembled nanoparticles. *Journal of Agricultural and Food Chemistry, 53*, 437–441.

Liu, Y., Hsu, C., Su, Y., & Lai, J. (2005). Chitosan–silica complex membranes from sulfonic acid functionalized silica nanoparticles for pervaporation dehydration of ethanol–water solutions. *Biomacromolecules, 6*, 368–373.

Mansouri, S., Lavigne, P., Corsi, K., Benderdour, M., Beaumont, E., et al. (2004). Chitosan–DNA nanoparticles as non-viral vectors in gene therapy: Strategies to improve transfection efficacy. *European Journal of Pharmaceutics and Biopharmaceutics, 57*, 1–8.

Mi, F. L., Sung, H. W., & Shyu, S. S. (2002). Drug release from chitosan–alginate complex beads reinforced by a naturally occurring cross-linking agent. *Carbohydrate Polymers, 48*, 61–72.

Muzzarelli, R. A. A. (1988). Carboxymethylated chitins and chitosans. *Carbohydrate Polymers, 8*, 1–21.

Muzzarelli, R. A. A., Tanfani, F., & Emanuelli, M. (1984). Chitin and its derivatives: New trends of applied research. *Carbohydrate Polymers, 3*, 53–75.

Nishimura, S. I., Kohgo, O., Kurita, K., & Kuzuhara, H. (1991). Chemospecific manipulations of a rigid polysaccharide: Syntheses of novel chitosan derivatives with excellent solubility in common organic solvents by regioselective chemical modifications. *Macromolecules, 24*, 4745–4748.

Peniche, C., Argüelles-Monal, W., Davidenko, N., Sastre, R., Gallardo, A., & Román, J. R. (1999). Self-curing membranes of chitosan/PAA IPNs obtained by radical polymerization: preparation, characterization and interpolymer complexation. *Biomaterials, 20*, 1869–1878.

Prashanth, K. V. H., Kittur, F. S., & Tharanathan, R. N. (2002). Solid state structure of chitosan prepared under different *N*-deacetylating conditions. *Carbohydrate Polymers, 50*, 27–33.

Qin, C., Du, Y., Zong, L., Zeng, F., Liu, Y., & Zhou, B. (2003). Effect of hemicellulase on the molecular weight and structure of chitosan. *Polymer Degradation and Stability, 80*, 435–441.

Rueda, D. R., Secall, T., & Bayer, R. K. (1999). Differences in the interaction of water with starch and chitosan films as revealed by infrared spectroscopy and differential scanning calorimetry. *Carbohydrate Polymers, 40*, 49–56.

Ruel-Gariépy, E., Shive, M., Bichara, A., Berrada, M., Le Garrec, D., Chenite, A., et al. (2004). A thermosensitive chitosan-based hydrogel for the local delivery of paclitaxel. *European Journal of Pharmaceutics and Biopharmaceutics, 57*, 53–63.

Santos, C., Mateus, M. L., Santos, A. P., Moreira, R., Oliveira, E., & Gomes, P. (2005). Cyclization-activated prodrugs. Synthesis, reactivity and toxicity of dipeptide esters of paracetamol. *Bioorganic and Medicinal Chemistry Letters, 15*, 1595–1598.

Sarmento, B., Ferreira, D., Veiga, F., & Ribeiro, A. (2006). Characterization of insulin-loaded alginate nanoparticles produced by ionotropic pre-gelation through DSC and FTIR studies. *Carbohydrate Polymers, 66*, 1–7.

Sato, H., Tsuge, S., Ohtani, H., Aoi, K., Takasu, A., & Okada, M. (1997). Characterization of chitin-based polymer hybrids by temperature-programmed analytical pyrolysis techniques. 1. chitin-graft-poly(2-methyl-2-oxazoline)/poly(vinyl chloride) blends. *Macromolecules, 30*, 4030–4037.

Skorik, Y. A., Gomes, C. A. R., Vasconcelos, M. T. S. D., & Yatluk, Y. G. (2003). *N*-(2-Carboxyethyl)chitosans: regioselective synthesis, characterisation and protolytic equilibria. *Carbohydrate Research, 338*, 271–276.

Skorik, Y. A., Gomes, C. A. R., Vasconcelos, M. T. S. D., Podberezskaya, N. V., Romanenko, G. V., Pinto, L. F., et al. (2005). Complexation models of *N*-(2-carboxyethyl)chitosans with copper(II) ions. *Biomacromolecules, 6*, 189–195.

Takeuchi, H., Thongborisute, J., Matsui, Y., Surihara, H., Yamamoto, H., & Kawashima, Y. (2005). Novel mucoadhesion tests for polymers and polymer-coated particles to design optimal mucoadhesive drug delivery systems. *Advanced Drug Delivery Reviews, 57*, 1583–1594.

Tapia, C., Escobar, Z., Costa, E., Sapag-Hagar, J., Valenzuela, F., Basualto, C., et al. (2004). Comparative studies on plyelectrolyte complexes and mixtures of chitosan-alginate and chitosan-carrageenan as prolonged diltiazem chlorhydrate release systems. *European Journal of Pharmaceutics and Biopharmaceutics, 57*, 65–75.

Thanou, M., Verhoef, J. C., Romeijn, S. G., Nagelkerke, J. F., Merkus, F. W. H. M., & Junginger, H. E. (1999). Effects of *N*-trimethyl chitosan chloride, a novel absorption enhancer, on Caco-2 intestinal epithelia and the ciliary beat frequency of chicken embryo trachea. *International Journal of Pharmaceutics, 185*, 73–82.

Thanou, M., Florea, B. I., Langemeÿer, M. W. E., Verhoef, J. C., & Junginger, H. E. (2000). *N*-Trimethylated chitosan chloride (TMC) improves the intestinal permeation of the peptide drug buserelin in vitro (caco-2 cells) and in vivo (rats). *Pharmaceutical Research, 17*, 27–31.

Thanou, M., Verhoef, J. C., Marbach, P., & Junginger, H. E. (2000). Intestinal absorption of octreotide: *N*-Trimethyl chitosan chloride (TMC) ameliorates the permeability and absorption properties of the somatostatin analogue in vitro and in vivo. *Journal of Pharmaceutical Sciences, 89*, 951–957.

Thanou, M., Verhoef, J. C., Verheijden, J. H. M., & Junginger, H. E. (2001). Intestinal absorption of octreotide using trimethyl chitosan chloride: Studies in pigs. *Pharmaceutical Research, 18*, 823–828.

Thierry, B., Kujawa, P., Tkaczyk, C., Winnik, F. M., Bilodeau, L., & Tabrizian, M. (2005). Delivery platform for hydrophobic drugs: Prodrug approach combined with self-assembled multilayers. *Journal of the American Chemical Society, 127*, 1626–1627.

Tian, F., Liu, Y., Hu, K., & Zhao, B. (2004). Study of the depolymerization behavior of chitosan by hydrogen peroxide. *Carbohydrate Polymers, 57*, 31–37.

Tirkistani, F. A. A. (1998). Thermal analysis of some chitosan Schiff bases. *Polymer Degradation and Stability, 60*, 67–70.

Vårum, K. M., Ottøy, M. H., & Smidsrød, O. (2001). Acid hydrolysis of chitosans. *Carbohydrate Polymers, 46*, 89–98.

Van der Merwe, S. M., Verhoef, J. C., Kotzé, A. F., & Junginger, H. E. (2004). *N*-trimethyl chitosan chloride as absorption enhancer in oral peptide drug delivery. Development and characterization of minitablet and granule formulations. *European Journal of Pharmaceutics and Biopharmaceutics, 57*, 85–91.

Vasconcelos, M. T. S. D., & Machado, A. A. S. C. (1986). Calibração do eléctrodo de vidro para determinação de constantes de formação em meio nem muito ácido nem muito alcalino (pH 4–10). *Revista Portuguesa de Química, 28*, 120.

Wong, K., Sun, G., Zhang, X., Dai, H., Liu, Y., He, C., et al. (2006). PEI-g-chitosan, a novel gene delivery system with transfection efficiency comparable to polyethyleneimine in vitro and after liver administration in vivo. *Bioconjugate Chemistry, 17*, 152–158.

Zhu, A. P., Ming, Z., & Jian, S. (2005). Blood compatibility of chitosan/heparin complex surface modified ePTFE vascular graft. *Applied Surface Science, 241*, 485–492.